Electrochimica Acta, Vol. 33, No. 6, pp. 753–760, 1988.
Printed in Great Britain.

0013–4686/88 $3.00 + 0.00

HYDROGEN AND OXYGEN EVOLUTION ON GRAPHITE FIBER–EPOXY MATRIX COMPOSITE ELECTRODES

S. M. LIPKA,*, G. L. CAHEN JR, G. E. STONER and L. L. SCRIBNER JR

Applied Electrochemistry Laboratory, Department of Materials Science, University of Virginia, Charlottesville, VA 22901, U.S.A.

and

E. GILEADI

School of Chemistry, Raymond and Beverly Sackler, Faculty of Exact Sciences, Tel Aviv University, Ramat Aviv 69978, Israel

(*Received* 11 *August* 1987; *in revised form* 28 *October* 1987)

Abstract—The electrochemical behavior of three graphite fiber–epoxy matrix composite materials containing various fiber orientations and fiber loadings was studied. Cyclic voltammetry was used to detect surface functionalities and to determine the electrochemically active surface areas of each material in 1 N H_2SO_4 and 30 weight percent (w/o) KOH.

Hydrogen and oxygen evolution were studied on each electrode in 1 N H_2SO_4 and 30 w/o KOH, respectively. Tafel slopes for the hydrogen evolution reaction on the composite electrodes ranged from 0.14 to 0.18 V decade^{-1} while exchange current densities ranged from 4 to 11 $\times 10^{-7}$ A cm^{-2}. Tafel slopes for the oxygen evolution reaction on the composite materials were high, ranging from 0.25 to 0.28 V decade^{-1}. Exchange current densities for the oxygen evolution reaction ranged from 2 to 5 $\times 10^{-7}$ A cm^{-2}. In general, fiber orientation and volume percent loading in the limited range studies had no noticeable effect on the kinetic behavior for the gas evolution reactions studied.

INTRODUCTION

Graphite fiber reinforced polymer matrix composites have been used in structural applications where high strength and modulus per unit weight are of prime importance. With a typical loading of 40–60 w/o of graphite fibers, these composites have sufficiently low electrical resistivity (ρ = 1–10 ohm cm) to allow their use as electrodes in a number of specific applications.

Graphite fiber–epoxy composite materials were first used by Stoner *et al.* [1, 2] as both the anode and the cathode in an *ac* electrochemical disinfection method developed earlier by Stoner[3]. These materials exhibit high structural stability and extended service life (compared to plain graphite employed in the earlier studies[3]) as long as the range of potentials is limited both anodically and cathodically to avoid copious gas evolution. It should be noted that the stability of graphite and graphite epoxy composite electrodes in solutions containing chloride ions under *ac* conditions is unique and cannot be matched by any of the metal electrodes in common use.

The properties of graphite fiber–polymer composite electrodes have been studied in recent years[4–7]. Stafford[5] characterized the electrochemical behavior and mechanical stability of composites having different polymer matrices (epoxybutadiene, polyester, epoxy and polyphenylene sulfide). It was observed that composites with lower impact resistance (epoxy and epoxybutadiene) were more stable electrochemically. Nacamulli and Gileadi[8] compared the behavior of glassy carbon to that of perpendicularly and randomly oriented graphite fiber–epoxy composite electrodes. Of the two composites, the one containing randomly oriented fibers yielded more reproducible results. The exchange current densities for oxygen evolution were in the range of 2–70 μA cm^{-2}, depending on the pH of the solution. The Tafel slopes were invariably high, in the range of 0.30–0.40 V decade^{-1}.

Other electrode blends of graphite and plastic material have been studied. These include electrodes made of graphite powder compressed in a Kel-F matrix[9–11] and reticulated vitreous carbon filled with epoxy[12, 13].

Since graphite fibers and graphite fiber–polymer composites are relatively new materials in electrochemistry, a study of their electrochemical properties was deemed appropriate. In the present work, composites having different loadings and orientations are compared.

EXPERIMENTAL

Electrode materials and fabrication

Three different graphite fiber–epoxy matrix composites were employed: A randomly oriented com-

* Present address: Physical Sciences, Inc., Research Park, P.O. Box 3100, Andover, MA 01810-7100, U.S.A.

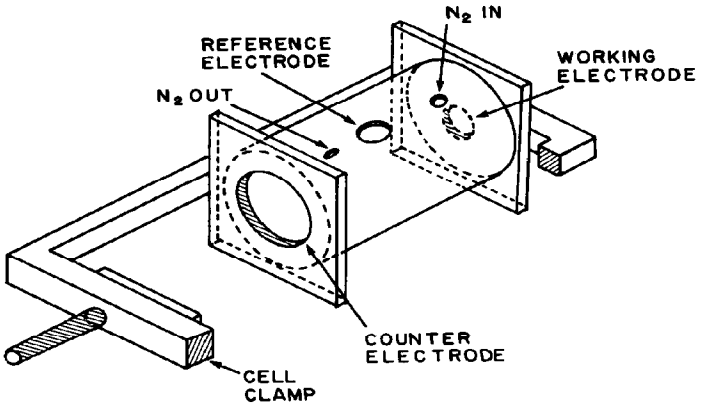

Fig. 1. The electrochemical cell.

posite (obtained from U.S. Polymeric, a division of Hitco, Santa Ana, CA) containing 38 volume percent (v/o), (50 w/o) pitch-based, 15 μm dia. fibers and a parallel oriented composite (obtained from Lockheed Corp. and containing Union Carbide Thornel 300 fibers). The latter contained PAN precursor fibers of 7 μm dia. with a loading of 50 v/o (65 w/o). This material was employed to make both the parallel and the perpendicular oriented fiber electrodes, by the appropriate machining of the electrode surfaces.

The composite electrodes were plated on the back side with nickel, employing a commercial nickel sulfamate bath (SEL-REX LECTRO-NIC 10–03 s) to ensure good electrical contact to the fibers*

Electrodes were polished with silicon carbide paper starting with 180 grit and finishing with 600 grit in several stages, with ultrasonic cleaning in distilled water between stages.

The cell and solutions

The cell used in these experiments is shown in Fig. 1. For use in 1 N H_2SO_4, a cell made of polymethylmathacrylate was employed. Experiments in 30 w/o KOH were conducted in a similar cell, made of PTFE. The exposed areas of the working and counter electrodes were 1 cm^2 and 5 cm^2, respectively. The two electrodes were 5.7 cm apart with a *sce* midway between them. Nickel plate was used as the counter electrode in alkaline solutions and Pt foil in acid solutions. The solutions in the cells were stirred with a magnetic stirrer and inlets and outlets for gas bubbling were provided. Solutions were made up from reagent grade chemicals and distilled water. The pH in the acid and alkaline solutions was 0.45 and 14.7 respectively.

Experimental procedures

A PAR model 173 Potentiostat, in combination with a Model 175 Universal Programmer was used for cyclic voltammetry. The current–potential curves were recorded either on an HP Model 7045A *X–Y* recorder or a Nicolet Explorer III Digital Storage Oscilloscope.

For steady-state galvanostatic measurements, the same potentiostat–galvanostat was used and the potential of the working electrode (with respect to a *sce* reference electrode) was measured using a Fluke Model 8810A Digital Multimeter. A current interruption method was used to determine and correct for the potential drop across the uncompensated part of the solution resistance in the course of galvanostatic measurements. The *sce* reference electrode was fitted with a small dia. (0.13 mm) Pt wire, which served as an auxiliary reference electrode for the measurement of the current interruption transient[14]. The *IR* correction employed was based on the average of four measurements at each current density.

The electrochemically active surface area was determined prior to each experiment from the double-layer capacitance obtained by cycling the electrode in the region where no Faradaic reaction occurred. A value of 20 μF was assumed per cm^2 of electrochemically active surface area. Following anodic polarization into the oxygen evolution region, the active surface area was determined before and after each experiment. The surfaces of the electrodes were also observed under an optical microscope and in the scanning electron microscope following each experiment.

All experiments were performed at ambient temperatures (23–25 °C). All potentials reported were measured *vs* a *sce*.

RESULTS AND DISCUSSION

Cyclic voltammetry and surface area determination

A typical cyclic voltammogram, obtained on a perpendicularly oriented graphite fiber–epoxy matrix composite electrode, in 1 N sulfuric acid, is shown in Fig. 2. The potential was scanned at 0.20 V s^{-1} between hydrogen evolution at *ca* −1.0 V *sce* (η = −0.72 V) and oxygen evolution at *ca* +1.45 V *sce* (η = +0.50 V). The voltammogram is mostly featureless,

*For the parallel oriented fibers, the edges of the fibers rather than the back side of the electrodes were plated.

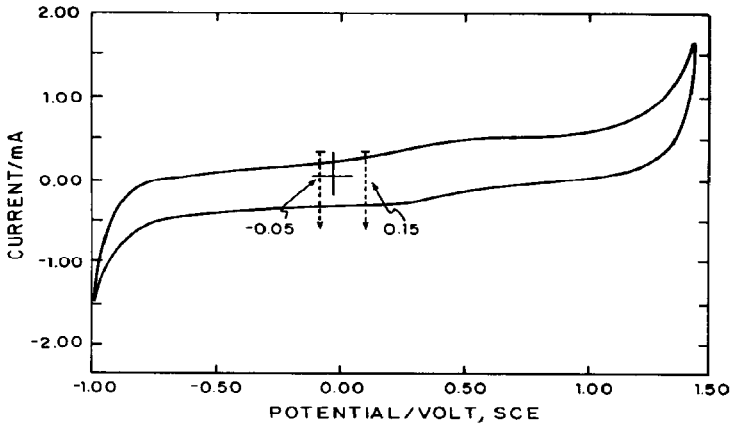

Fig. 2. Cyclic voltammogram at perpendicularly oriented composite electrode in deaerated 1 N H_2SO_4. Scan rate 0.20 V s^{-1}. Limits of potential: −1.00 to +1.5 V, *sce*.

with small anodic and cathodic currents in the range of 0.30–0.60 V *sce*, which can be associated with the oxidation and reduction of surface functional groups on graphite. Similar results were also observed on the other composite electrodes, in agreement with an earlier observation on randomly oriented composites[8], and the occurrence of anodic and cathodic peaks on cyclic voltammograms of graphitic materials has been widely reported in the literature[15–22].

For the determination of the real surface area from double-layer capacity measurements, it is necessary to identify a potential region in which no Faradaic reaction occurs. Considering the cyclic voltammogram in Fig. 2, it is seen that no "true" double-layer region exists in this system. To find a potential region most suitable for this measurement, a window of potential of 0.20 V was chosen, and this window was examined for the whole range of potential studied. The region of −0.050 to +0.150 V *sce* was chosen, on the basis of three criteria: no oxidation–reduction peaks, lowest anodic and cathodic currents, and approximate symmetry of the anodic and cathodic currents around zero. The resulting current–potential plots over the limited range of potentials chosen are given in Fig. 3 for a number of sweep rates. The same data (obtained for a parallel oriented composite electrode) are plotted in Fig. 4 as the charging current *vs* the sweep rate. Good linear relationship is observed (correlation coefficient 0.9995). The capacity per cm^2 of geometrical surface area is found to be *ca* 84 μF. The results obtained in the same manner for different electrode materials in 1 N H_2SO_4 are listed in Table 1. The roughness factors were calculated assuming a capacitance of 20 $\mu F\,cm^{-2}$ of true surface area. It is recognized that this value is rather arbitrary, and indeed, the differences between the roughness factors calculated from measurements in acid and alkaline may well be due to a difference in double-layer capacitance per unit area rather than to a difference in actual roughness of the electrodes exposed to the two solutions. The values calculated can nevertheless serve to compare different graphite materials and to observe any changes in surface roughness

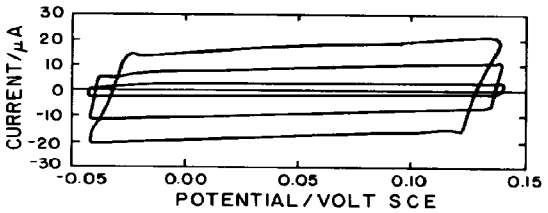

Fig. 3. Cyclic voltammograms in a limited potential region (−0.05 to +0.15 V, *sce*) for a randomly oriented composite in deaerated 1 N H_2SO_4. Sweep rates shown 20; 100; 200 mV s^{-1}.

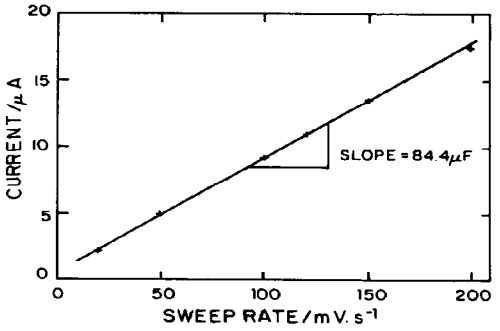

Fig. 4. The double layer charging current as a function of sweep rate for the system shown in Fig. 3.

which may be caused by chemical or electrochemical treatments.

A cyclic voltammogram obtained on a randomly oriented composite electrode in 30 w/o KOH is shown in Fig. 5. The cathodic and anodic limits in this case were −1.70 and +0.60 V *sce*, corresponding to overpotentials of *ca* −0.60 and 0.50 V respectively, somewhat less than in 1 N H_2SO_4. The voltammograms

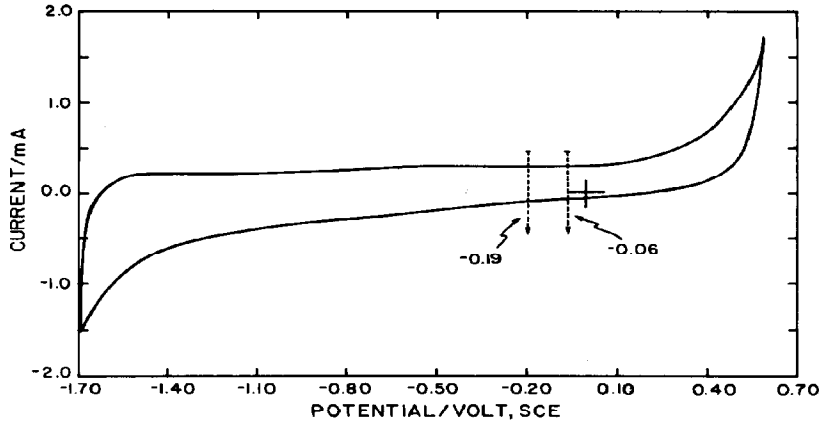

Fig. 5. Cyclic voltammogram at a randomly oriented composite electrode in deaerated 30 w/o KOH. Scan rate 0.20 V s^{-1}. Limits of potential: −1.70 to +0.60 V, *sce*.

observed in this solution on all electrode materials tested were almost smooth between the extremes of hydrogen and oxygen evolution, and peaks for oxidation and reduction of surface species could barely be detected. The best potential window for double-layer capacitance measurements in this solution was −0.19 to −0.060 V *sce*. The current potential behaviour in this region is shown in Fig. 6, for a number of sweep rates. The results of such measurements for all electrode materials tested are shown in Table 2. Polarizing the electrode anodically in the oxygen-evolution region is seen to cause an increase in the measured capacitance for random and perpendicular oriented composites. Although a roughness factor was calculated in each case (based on the assumed 20 μF cm^{-2}) it cannot be stated with certainty that the whole increase in the measured capacity is due to a proportional increase in surface roughness, since oxidation of the surface probably occurs during anodic polarization and this may cause a change in double-layer capacitance per unit surface area*.

Kinetics of hydrogen evolution

The kinetic behavior of the hydrogen evolution reaction was studied galvanostatically in 1 N H_2SO_4 at the different electrodes used in this work. The current densities were calculated on the basis of surface areas determined from the measured capacitance, as described above. Measured potentials were corrected for *IR* drop over the uncompensated part of the solution resistance. Tafel slopes for the three types of composites used in the present study are shown in Fig. 7. Linear behavior is observed over *ca* three decades of current density for all three electrodes, and the values of the Tafel slopes observed are larger than

* For example, the potential of zero charge may be shifted. Thus, while the potential is maintained constant with respect to a reference electrode, its value on the so called "rational scale" may change, leading to a change in the numerical value of the double-layer capacitance.

Table 1. Double-layer capacitance C_{dl} and roughness factors for different electrode materials in 1 N H_2SO_4

Electrode	Double-layer C_{dl} (μF)	Calculated roughness factor
Graphite–epoxy composite (random, 38 v/o)	141	19*
Graphite–epoxy composite (perpendicular, 50 v/o)	190	19†
Graphite–epoxy composite (parallel, 50 v/o)	84	8.4†

* Assuming that 38% of the surface contains conducting graphite fibers.
† Assuming that 50% of the surface contains conducting graphite fibers.

0.12 V $decade^{-1}$. The calculated Tafel slopes and exchange current densities are shown in Table 3. A study of the mechanism of hydrogen evolution on these materials was not attempted. The exchange current densities are intermediate between those found for catalytic metals (Pt, Ni) and those observed for "soft" metals (Hg, Pb). The interplay between the values of i_0 and b in determining the catalytic activity of an electrode material is clearly demonstrated in Fig. 7 and Table 3. Thus, i_0 is *ca* three times higher for the parallel oriented composite than for the perpendicularly oriented one, yet at an overpotential of $\eta = -0.40$ V the situation reverses and the current density on the perpendicularly oriented composite is about three times larger. Indeed, the comparison of the catalytic activity of different electrode materials for a given reaction in terms of their respective exchange current densities is straightforward only if the Tafel slopes are equal. In complex cases such as the one considered here, the catalytic activity might best be assessed, from an engineering point of view, by comparing the overpotentials in the range of current densities of practical interest. Since the Tafel lines for the parallel and perpendicular oriented composites cross over at a current density of *ca* 10 μA cm^{-2}, the perpendicular

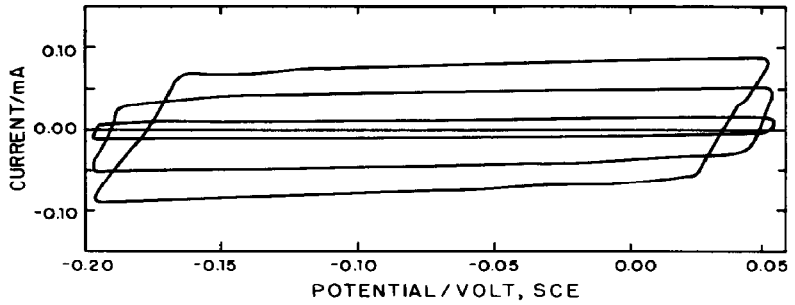

Fig. 6. Cyclic voltammograms in a limited potential region (-0.19 to -0.06 V, *sce*) for a perpendicularly oriented composite in deaerated 30 w/o KOH. Sweep rates shown: 20, 100: 180 mV s^{-1}.

Table 2. Double-layer capacitance and roughness factors for different electrode materials in 30 w/o KOH before and after oxygen evolution

Electrode	Before oxygen evolution C_{dl} (μF)	Before oxygen evolution Calculated roughness factor	After oxygen evolution C_{dl} (μF)	After oxygen evolution Calculated roughness factor	Percent change
Graphite–epoxy composite (random, 38 v/o)	172	23 *	726	96 *	321
Graphite–epoxy composite (perpendicular, 50 v/o)	249	25 †	409	41 †	64
Graphite–epoxy composite (parallel, 50 v/o	289	29 †	188	19 †	−35

* Assuming that 38% of the surface contains conducting graphite fibers.
† Assuming that 50% of the surface contains conducting graphite fibers.

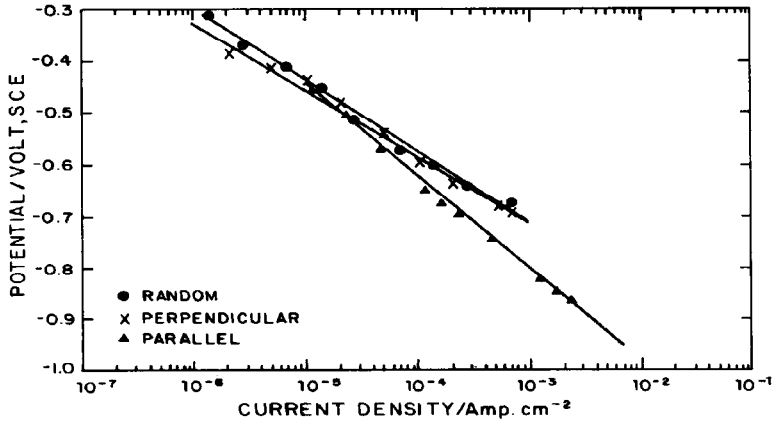

Fig. 7. Tafel plots for three types of composite electrodes in deaerated 1 N H_2SO_4.

oriented material should be considered more catalytic, from a practical standpoint.

The composite electrodes showed no changes in surface morphology as a result of hydrogen evolution, when viewed by optical microscopy. This is consistent with earlier findings of Stafford[5] and with the fact that overpotentials measured at a given current density were not affected by polarization to higher cathodic current densities in the hydrogen evolution region.

Kinetics of oxygen evolution

Oxygen evolution was studied in concentrated alkaline solutions (30 w/o KOH). It has been rep-

Table 3. Kinetic parameters for hydrogen evolution in deaerated H_2SO_4

Electrode	Tafel slope (b_c)/V	Exchange current density (i_0) (A cm^{-2})
Graphite–epoxy composite (random, 38 v/o)	−0.14	6×10^{-7}
Graphite–epoxy composite (perpendicular, 50 v/o)	−0.13	4×10^{-7}
Graphite–epoxy composite (parallel, 50 v/o)	−0.18	11×10^{-7}

Table 4. Kinetic parameter for oxygen evolution in deaerated 30 w/o KOH

Electrode	Tafel slope (b_a)/V	Exchange current density (i_0) (A cm^{-2})
Graphite–epoxy composite (random, 38 v/o)	+0.27	2×10^{-7}
Graphite–epoxy composite (perpendicular, 50 v/o)	+0.25	3×10^{-7}
Graphite–epoxy composite (parallel, 50 v/o)	+0.28	5×10^{-7}

orted[5] that carbon fiber–epoxy matrix composite electrodes undergo partial oxidation when polarized anodically. This may cause a change in surface roughness, as shown in Table 2. The real surface area used for plotting the Tafel line for oxygen evolution and calculating the exchange current densities were based on double-layer capacitance measurements taken after the galvanostatic polarization curve has been determined. Repeating the measurements on the same electrode leads, as a rule, to a parallel shift of the Tafel line to somewhat lower overpotentials, consistent with the assumption of increasing surface area as a result of high anodic polarization.

Tafel lines obtained on the three composite electrodes are shown in Fig. 8 and the corresponding calculated Tafel slopes and exchange current-densities are presented in Table 4. It is noted that the Tafel lines for both hydrogen and oxygen evolution observed in this work (Figs 7 and 8, respectively) are linear over 2–3 decades of current density, corresponding to 0.4–0.8 V. Thus, the experimentally observed transfer coefficient, α, is independent of potential over a relatively wide range. On the other hand, the values observed for oxygen evolution ($\alpha = 0.24$) are lower than those commonly reported for charge transfer across the Helmholtz layer. Values of $\alpha < 0.5$ can be rationalized in terms of surface-film formation (*eg* the anodic oxide film on Al or the solid electrolyte interphase formed at Li electrodes in nonaqueous media), with part of the potential drop occuring across such a film. This may be the cause for the low values of α (*ie* high Tafel slopes) observed here, although direct evidence of film formation has not been generated.

The Tafel slopes and exchange current densities on all three composite electrodes are close and probably within experimental error.

Scanning electron micrographs of a perpendicular oriented graphite fiber–epoxy matrix composite following anodic oxidation are shown in Fig. 9. In Fig. 9a the dark areas around and in the middle of the fibers correspond to regions where the graphite has been removed by oxidation. Figure 9b represents a later stage in the oxidation process. The fibers are seen to have receded, leaving behind a honeycomb type structure of tubular holes in the epoxy matrix.

CONCLUSIONS

Hydrogen and oxygen evolution have been studied in acid and alkaline media, respectively, on graphite fiber–epoxy matrix composite electrodes. Three types of fiber orientation composites were tested: random, parallel and perpendicular to the electrode surface. Linear Tafel behavior was observed in all cases over a range of 2.5–3.0 decades in current density. The Tafel

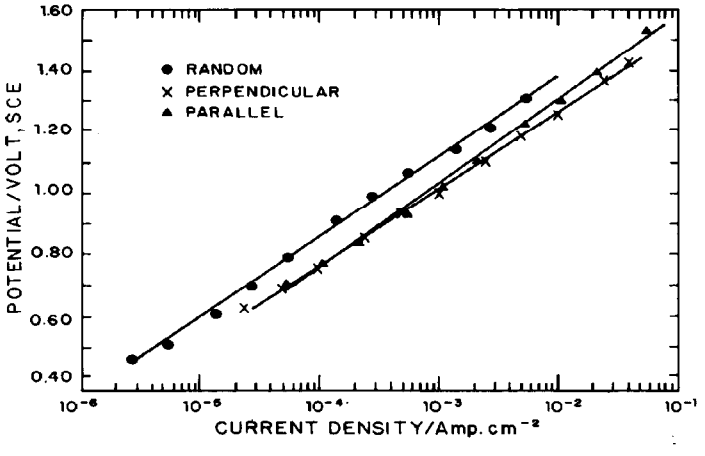

Fig. 8. Tafel plots for three types of composite electrodes in deaerated 30 w/o KOH.

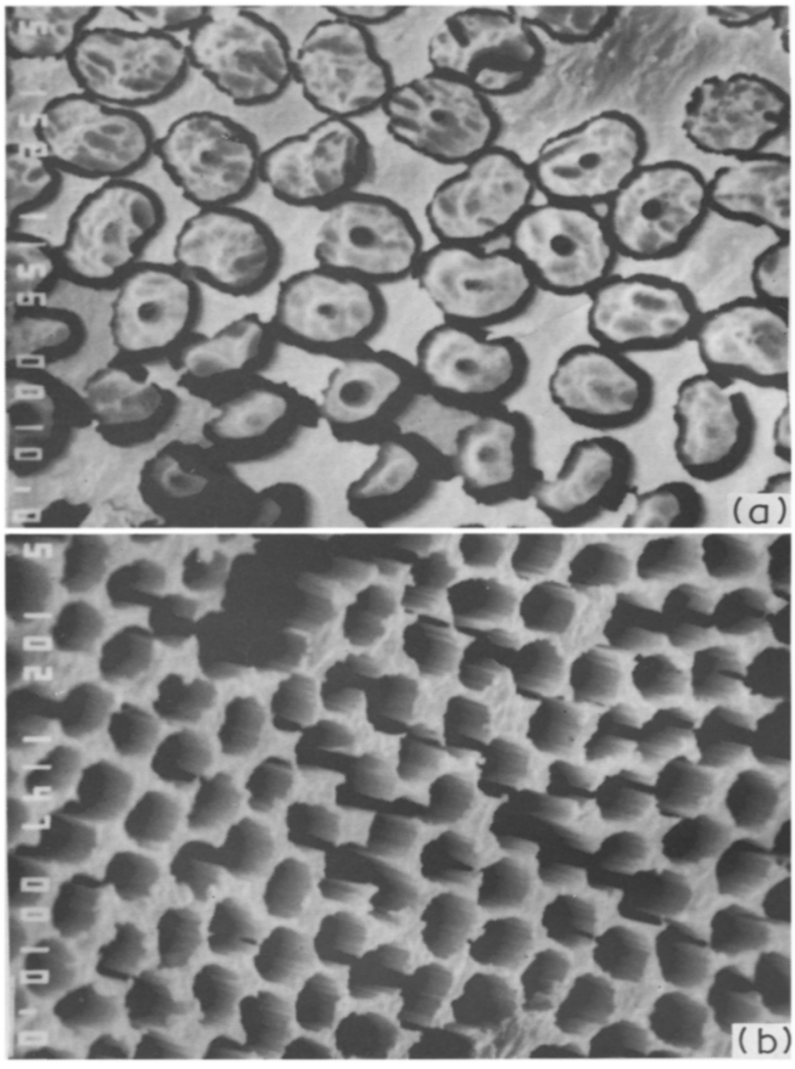

Fig. 9. Scanning electron micrograph of perpendicularly oriented composite following anodic oxidation. (a) Moderate oxidation. (b) Extensive oxidation.

slopes observed are high (significantly more than 0.12 V decade^{-1} in all cases) pointing to a complex behavior, possibly involving surface films and electroactive species covalently bound to the surface.

The electrodes are poor catalysts for the water decomposition reaction. This is shown by the low values of the exchange current densities for both hydrogen and oxygen evolution and the wide range of potentials observed during cyclic voltammetry (typically 2.3–2.5 V) between substantial oxidation and reduction of the solvent. The electrodes are stable during hydrogen evolution but are oxidized at anodic potentials in the course of oxygen evolution.

Small Faradaic currents are observed during cyclic voltammetry between hydrogen and oxygen evolution. This is due to oxidation–reduction processes of chemically bonded, oxygen containing species, which have been reported previously in a number of publications. By limiting the potential span to 0.1–0.2 V, it is possible to find a window on the potential scale in which the currents are essentially non-Faradaic, allowing a determination of the double-layer capacitance and from it the roughness factor.

Acknowledgement—Financial support by the U.S. Army Research Office (grant No. DAAG29-82-K-0053) is gratefully acknowledged.

REFERENCES

1. S. C. Hendrickson, M.S. Thesis, UVA, May (1978).
2. G. E. Stoner, G. L. Cahen, Jr., M. Sachyani and E. Gileadi, *Bioelectrochem. Bioenerg.* **9**, 229 (1982).
3. G. E. Stoner, U.S. Patent No. 3, 725, 266 (1973).

4. G. L. Cahen, D. J. Kirwan, J. W. Parcells and G. E. Stoner, Abstract No. 442, Extended Abstracts, Vol. 81-1, ECS Spring Meeting, Minneapolis, Minnesota, May (1981).
5. G. R. Stafford, Ph.D. Thesis, UVA, May 1980, G. R. Stafford, G. E. Stoner and G. L. Cahen Jr, *J. electrochem. Soc.* (submitted).
6. R. C. Paciej, M.S. Thesis, UVA, May 1982.
7. P. M. Natishan, Ph.D. Thesis, UVA, January (1984).
8. L. Nacamulli and E. Gileadi, *J. appl. electrochem.* **12,** 73, (1982).
9. J. E. Anderson, D. E. Tallman, D. J. Chesney, and J. L. Anderson, *Anal. Chem.* **50,** 1051, (1978).
10. D. E. Weisshaar and D. E. Tallman, *Anal. Chem.* **53,** 1809, (1981).
11. D. E. Weisshaar and D. E. Tallman, *Anal. Chem.* **55,** 1146, (1983).
12. N. Sleszynski and J. Osteryoung, Abstract No. 382, Extended Abstracts, Vol. 84-1, ECS Spring Meeting, Cincinnati, OH, May (1984).
13. N. Sleszynski and J. Osteryoung, *Anal. Chem.* **56,** 130, (1984).
14. P. J. Moran, Ph.D. Thesis, UVA, January 1980.
15. K. F. Blurton, *Electrochim. Acta,* **18,** 869, (1973).
16. J. P. Randin and E. Yeager, *J. electroanal. Chem.* **58,** 313, (1975).
17. V. A. Garten and D. E. Weiss, *Aust. J. Chem.* **8,** 68, (1955).
18. B. D. Epstein, E. Dalle-Molle and J. S. Mattson, *Carbon* **9,** 609, (1971).
19. J.V. Hallum and H. V. Drushel, *J. phys. Chem.* **62,** 110, (1958).
20. J. V. Hallum and H. V. Drushel, *J. phys. Chem.* **62,** 1502 (1958).
21. H. Alt, H. Binder, A. Kohling and G. Sandstede, *Angew Chem. Internat. Edn.* **10,** 514, (1971).
22. H. Alt, H. Binder, A. Kohling and G. Sandstede, *Electrochim. Acta* **17,** 873, (1972).